Osteoporosis International (2020) 31:941–950
https://doi.org/10.1007/s00198-020-05298-z

ORIGINAL ARTICLE

Comparison of bone structure and microstructure in the metacarpal heads between patients with psoriatic arthritis and healthy controls: an HR-pQCT study

D. Wu[1] · J.F. Griffith[2] · S.H.M. Lam[1] · P. Wong[1] · J. Yue[1] · L. Shi[3] · E.K. Li[1] · I.T. Cheng[1] · T.K. Li[1] · V.W. Hung[4] · L. Qin[4] · L.-S. Tam[1]

Received: 6 June 2019 / Accepted: 10 January 2020 / Published online: 14 January 2020

Abstract

Summary Human cadaveric study has indicated that the metacarpal head (MCH) is intracapsular in location. We hypothesized that exposure to the intra-articular inflammatory milieu in psoriatic arthritis (PsA) will lead to bone loss in the MCH.

Introduction To compare the bone structure and microstructure in the MCH between patients with PsA and healthy controls by high-resolution peripheral quantitative CT (HR-pQCT), and to ascertain factors associated with bone loss in PsA patients.

Methods Sixty-two PsA patients without joint destruction and 62 age-, gender-, and body mass index–matched healthy subjects underwent HR-pQCT imaging of the second and third MCH (MCH 2&3). The number and volume of bone erosion and enthesiophytes, as well as volumetric bone mineral density (vBMD) and microstructure at the MCH 2&3, were recorded. Correlation analysis and multivariable linear regression models were used to determine the association of demographic and disease-specific variables with compromised bone structure and microstructure in PsA.

Results At the MCH 2&3, bone erosion ($p = 0.003$) and enthesiophyte ($p = 0.000$) volumes in PsA patients were significantly larger than healthy controls. In PsA patients, older age was associated with a larger erosion and enthesiophyte volume. Concerning the mean vBMD and microstructure at the MCH 2&3, PsA patients had significantly lower mean vBMD (average vBMD −6.9%, trabecular vBMD −8.8%, peri-trabecular vBMD −7.7%, meta-trabecular vBMD −9.8%), trabecular bone volume fraction (−8.8%), and trabecular thickness (−8.1%) compared with control subjects. Multivariable regression analysis revealed that older age and a higher C-reactive protein level were associated with trabecular bone loss.

Conclusions PsA patients had a higher burden of bone damages (erosions and enthesiophytes) and trabecular bone loss compared with healthy control at the MCH. Inflammation contributed to the deterioration in trabecular microstructure in these patients.

Keywords Bone erosion · Enthesiophyte · HR-pQCT · Psoriatic arthritis

Electronic supplementary material The online version of this article (https://doi.org/10.1007/s00198-020-05298-z) contains supplementary material, which is available to authorized users.

✉ L.-S. Tam
lstam@cuhk.edu.hk

[1] Department of Medicine & Therapeutics, The Prince of Wales Hospital, The Chinese University of Hong Kong, Hong Kong, China

[2] Department of Imaging and Interventional Radiology, The Prince of Wales Hospital, The Chinese University of Hong Kong, Hong Kong, China

[3] Research Centre for Medical Image Computing, Department of Imaging and Interventional Radiology, The Prince of Wales Hospital, The Chinese University of Hong Kong, Hong Kong, China

[4] Bone Quality and Health Centre of the Department of Orthopedics & Traumatology, The Prince of Wales Hospital, The Chinese University of Hong Kong, Hong Kong, China

Introduction

Psoriatic arthritis (PsA) is a chronic inflammatory arthritis characterized by synovitis and enthesitis [1–3]. Inflammatory arthritis, including rheumatoid arthritis (RA) and PsA, leads to structural damage at the metacarpophalangeal joint [4, 5]. High-resolution peripheral quantitative computed tomography (HR-pQCT) enables the assessment of bone erosions, new bone formation, and cortical and trabecular microarchitecture [6]. HR-pQCT-based studies have shown that entheseal new bone formation is an early sign of bone change in PsA [7, 8]. This entheseal new bone formation represents a dominant structural feature of disease in established PsA which is largely absent in RA [4]. Much of the structural change seen in PsA seems to be

driven by entheseal inflammation [4]. Erosions, on the other hand, reflect mechanical and inflammatory joint damage and are more prevalent in RA rather than PsA [4]. An HR-pQCT-based study has demonstrated that tumor necrosis factor (TNF) inhibition arrests the progression of bone erosion but not enthesiophye formation [9], while interleukin (IL)-17 inhibition arrests the progression of both bone erosion and enthesiophyte formation [10], suggesting fundamental differences in the pathophysiology of bone erosions and enthesiophytes.

The entire metacarpal head (MCH) is located inside the joint capsule and is therefore exposed to the intra-articular inflammatory milieu in inflammatory arthritides [11]. Within the MCH, bone loss has been found in both the trabecular and cortical compartments in RA patients [11]. Whether the predominantly entheseal-driven inflammatory process of PsA is associated with intra-articular bone loss similar to that seen in RA patients is uncertain. Our aims were (1) to compare the intra-articular bone structure and microstructure between PsA patients and healthy control subjects; and (2) to ascertain the demographic and clinical factors associated with compromised bone microstructure in PsA patients.

Methods

Patients

Seventy-seven PsA patients and 62 healthy controls were studied in this cross-sectional study. Distal radial densitometric and microstructural features in 53 of the 77 PsA patients and 53 of the 62 controls were published previously [12]. All PsA patients fulfilled the ClASsification for Psoriatic ARthritis (CASPAR) criteria [13] and were recruited from the Rheumatology Clinic at the Prince of Wales Hospital. Exclusion criteria for patients were as follows: (1) HR-pQCT image showing joint destruction (bone erosions and enthesiophytes leading to destruction of the normal joint structure, sFigure 1) [14]; (2) presence of an underlying disorder that could affect bone metabolism such as chronic renal impairment (chronic kidney disease stage IV or V), type 1 diabetes mellitus (DM), unstable cardiovascular disease, thyroid or parathyroid disease, malignancy, or chronic liver disease; (3) current or past usage of anticonvulsant therapy, thyroid or parathyroid hormone, or antiosteoporosis therapy; and (4) pregnancy or breastfeeding. Treatment with glucocorticoids, calcium, and/or vitamin supplement was allowed. After PsA patients with joint destruction were excluded, sixty-two age- and sex-matched healthy control subjects were selected from our previous study (sFigure 2) [12]. Exclusion criteria for control subjects include all of the above exclusion criteria, as well as a history of any autoimmune disease or any other major illness, with the exception of hypertension, type II DM, and dyslipidemia. Ethics approval (CRE-2012.082) was obtained from the Ethics Committee of The Chinese University of Hong Kong-New Territories East Cluster Hospitals with written informed consent obtained from all participants.

Clinical assessment

Age, body weight, body height, and smoking habit were recorded and body mass index (BMI) was calculated for all participants. Clinical assessment performed by rheumatologists included the number of tender (0–68) and swollen (0–66) joints, permanently deformed joints and the presence of dactylitis. Psoriatic nail involvements, including pitting, hyperkeratosis, and onycholysis, were assessed. The levels of erythrocyte sedimentation rate (ESR) and C-reactive protein (CRP) were measured. Disease activity was assessed using the Disease Activity index for PsA (DAPSA) [15] and Psoriasis Area and Severity Index (PASI); while physical function was assessed using the Health Assessment Questionnaire (HAQ) disability index. Also recorded were the presence of rheumatoid factor (RF), current use of conventional synthetic disease-modifying anti-rheumatic drugs (csDMARDs), non-steroidal anti-inflammatory drugs (NSAIDs), and biologic DMARDs (bDMARDs).

High-resolution peripheral quantitative CT

All patients underwent an HR-pQCT (Xtreme-CT scanner, Scanco Medical AG, Brüttisellen, Switzerland) examination of the second and third MCH (MCH 2&3) of the non-dominant forearm [12]. The patient's forearm was immobilized in a carbon fiber cast fixed within the scanner gantry. A dorso-palmar projection image was obtained to define the tomographic scan plane. The scan region started at the distal end of the MCH 2&3 and spanned proximally 9.02 mm (110 slices).

Detection of erosion and enthesiophyte

MCH 2&3 was divided into palmar, ulnar, dorsal, and radial quadrants [14, 16] to evaluate the number and size of erosions and enthesiophytes within each quadrant (sFigure 3). Erosions were defined as a clear break in the outer cortical margin evident on at least two consecutive slices and in two orthogonal planes [4, 7, 14]. A cortical break was considered a vascular channel if it was tubular in outline, regularly delineated, without loss of surrounding trabecular structure [17–19]. Pseudo-erosions formed by two osteophytes configured like an open forceps were excluded [20]. To increase the specificity of identifying pathological erosions, only cortical breaks wider than 1.9 mm [14] were included for further analysis.

Enthesiophytes were defined as new bone formation arising from the periosteal bone cortex at the insertion sites of the capsule, ligament, or tendons or at the location of functional enthesis [7, 21]. The maximal distance between the superficial surface of the enthesiophyte and the missing true cortical boundary was defined as the maximal height (mm) (sFigure 4) [4, 5, 7, 21]. Erosions and enthesiophytes were identified and evaluated by two independent, blinded readers (DZW, SHL). When more than one erosion or enthesiophyte was present in a single quadrant, the one with the largest volume or height was selected [7].

Image analysis for erosion and enthesiophyte at the second and third metacarpal head

Images were analyzed using the open-source application ITK-SNAP interactive image visualization and segmentation tool [22–24], validated for volume measurement of hard and soft tissue [24–28]. The technique comprised four major steps: (1) metacarpal bone cropping, (2) periosteal surface segmentation, (3) restoration of the missing true periosteal cortical boundary, and (4) volume calculation (Fig. 1A, B). Periosteal surface restoration was performed using a threshold-based semi-automatic segmentation method with supervised learning [23]. Any missing periosteal cortex margin was manually restored based on the anatomic curve. Restoration of the periosteal cortical margin was an important step in the analytical process given that enthesiophytes and erosions were bone deposited on and resorbed from the periosteal cortical margin respectively [29]. As determined by intraclass correlation coefficient (ICC), inter-observer reliability for bone erosion volume was 0.996 (95%CI: 0.992, 0.998) and for enthesiophyte maximal height and volume were 0.741 (95%CI: 0.419, 0.885) and 0.986 (95%CI: 0.968, 0.994).

Image analysis for vBMD and microstructure at the second and third metacarpal head

MCH 2&3 were chosen as they are the most commonly affected finger joints among MCH 2–4, [4]. Images were analyzed using a standard protocol provided by the manufacturer [30] after exclusion of bone erosion and enthesiophyte (Fig. 1C, D) [31]. The following parameters were measured: average vBMD, trabecular (Tb) vBMD, meta-trabecular (mTb, inner 60% of the medullary region) vBMD, peri-trabecular (pTb, outer 40% of the medullary region) vBMD. Trabecular bone structure was evaluated by determining the trabecular bone volume fraction (BV/TV), trabecular number, thickness, separation, and trabecular inhomogeneity (standard deviation of 1/trabecular number). Cortical bone vBMD, thickness, and perimeter were also measured. Our short-term HR-pQCT reproducibility, expressed as coefficient of variance, ranges from 0.38 to 1.03% for density measures and from 0.80 to 3.73% for microstructural measures [32].

Statistical analysis

Data are presented as number (percentage) for categorical data, mean ± SD for normally distributed data, or median and interquartile range (IQR) for non-normally distributed data. Normality testing was performed using a combination of Kolmogorov-Smirnov test and histogram. Differences between PsA patients and controls in terms of demographic and HR-pQCT parameters (erosion and enthesiophyte [total number and total volume at MCH 2&3], mean vBMD, and bone microstructure at MCH 2&3) were assessed using the chi-square test for categorical variables, Mann–Whitney *U* test, or Student's *t* test for continuous variables depending on the data distribution. In PsA patients, Pearson's and Spearman's correlation analyses were used to determine the association between demographic and clinical characteristics (age, psoriasis and PsA disease duration, BMI, CRP and DAPSA) and HR-pQCT parameters (erosion and enthesiophyte volume, vBMD, and bone microstructure) for normally or non-normally distributed data respectively. Potential variables associated with microstructural measures were examined first by univariate correlation analysis and subsequently by multiple linear regression analysis. Independent explanatory variables associated with compromised microstructure in PsA were assessed using multivariable linear regression models with adjustment for covariates (including all the potential explanatory variables associated with compromised microstructure identified from the univariate analyses with a p value < 0.05). A histogram was used to show the anatomic distribution of bone erosion and enthesiophyte. A p value of < 0.05 was considered statistically significant throughout the analysis. All statistical analyses were performed using the Statistics Package for Social Sciences (IBM SPSS V.21.0, IBM Corporation, Armonk, NY, USA).

Results

Demographic and clinical features

Fifteen out of 77 (19.5%) PsA patients were excluded due to joint destruction. The remaining 62 patients and 62 healthy control subjects were comparable for gender, age, body mass index (BMI), and smoking habit (Table 1). PsA disease duration was 17.3 ± 14.5 years, with a low to moderate disease

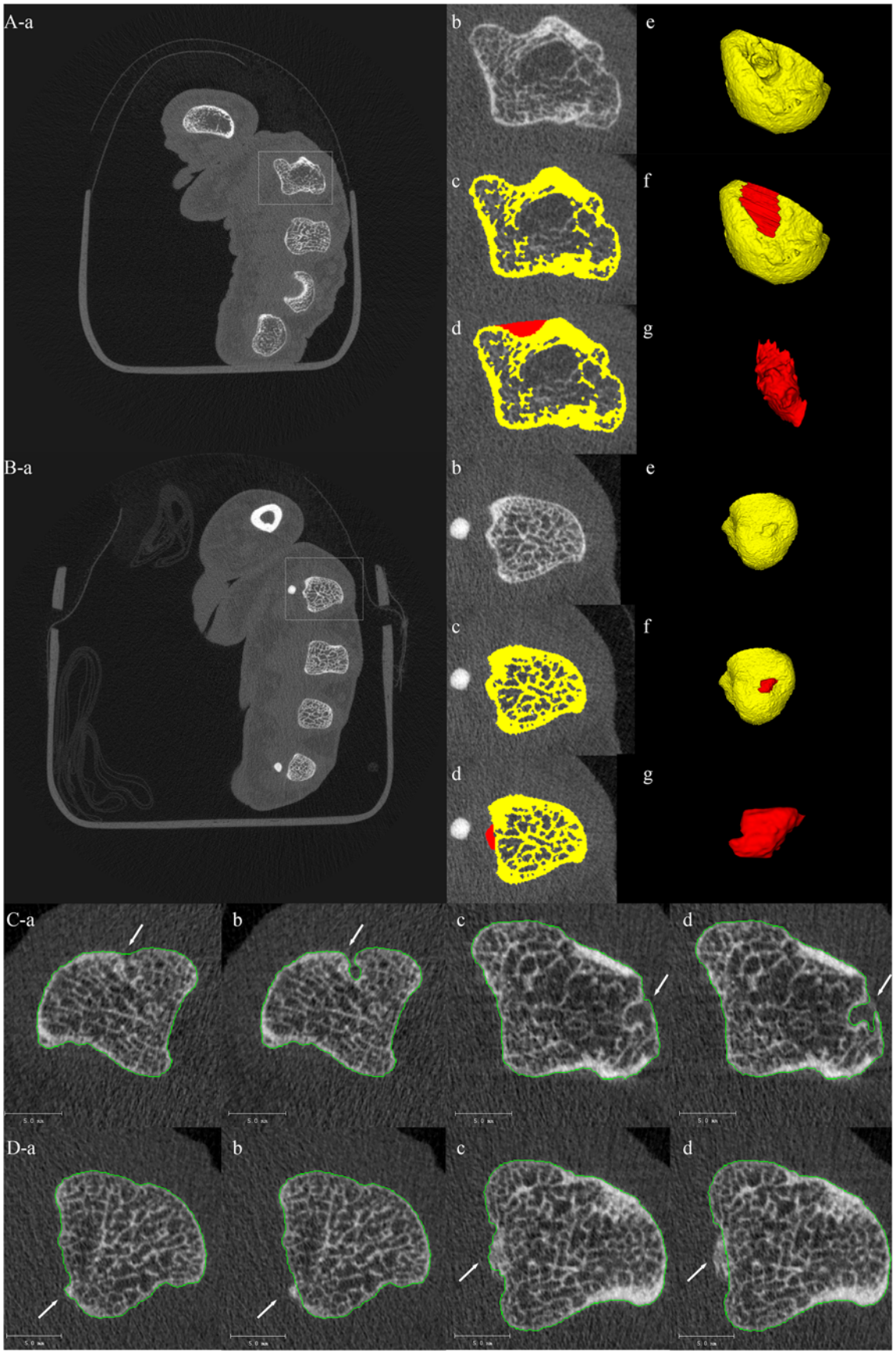
A-a
b
c
d
e
f
g
B-a
b
c
d
e
f
g
C-a
b
c
d
D-a
b
c
d

◀ **Fig. 1** Image analysis on structural and microstructural bone changes. Quantification of bone erosion or enthesiophyte volume (A, B): crop of metacarpal bone (a, b), segmentation of periosteal surface (c, e), restoration of the missing true cortical boundary based on anatomic curve, (d, f), and three-dimensional calculation of volume (g). Calculation of bone density and microstructure after the exclusion of bone erosion and enthesiophyte (C, D): contour before exclusion of bone erosion and enthesiophyte (a, c) and contour after exclusion of bone erosion and enthesiophyte (b, d)

activity (DAPSA: 10.8 ± 8.1; ESR: 20.5 ± 20.6 mm/h; CRP: 5.2 ± 8.4 mg/L). Three (4.8%), 33 (53.2%), and 11 (17.7%) patients were receiving corticosteroids, conventional synthetic disease-modifying anti-rheumatic drugs (csDMARDs), and biologic DMARDs respectively. None of the patients had a positive RF.

Comparison of bone structure at the second and third metacarpal heads in PsA and controls

All subjects except one (a PsA patient) had at least one bone erosion. In the PsA group, 85 erosions were identified, while only 50 erosions were observed in the control group. At MCH 2&3, the mean number of erosion (PsA: 1.4 ± 1.2 vs control: 1.1 ± 1.0, $p = 0.110$) was similar between the two groups, yet the total erosion volume per person was significantly greater in PsA compared with controls (PsA: 5.2 ± 6.0 mm^3 vs control: 2.8 ± 4.5 mm^3, $p = 0.003$) (Table 2). Bone erosion in PsA patients had a typical predilection for the radial and dorsal site (Fig. 2A).

Four PsA patients and 15 healthy controls had no enthesiophyte. In the PsA group, 150 enthesiophytes were identified, while only 80 enthesiophytes were observed in

Table 1 Demographic and clinical characteristics of patients with psoriatic arthritis and controls

	PsA without JD ($n = 62$)	Controls ($n = 62$)	p value[#]
Demographic characteristics			
Female, %	28 (45.2)	31 (50.0)	0.590
Age, year	52.94 ± 11.5	50.8 ± 9.3	0.265
BMI	25.2 ± 4.1	24.0 ± 3.0	0.077
Height, cm	163.2 ± 8.1	162.7 ± 7.1	0.708
Weight, kg	67.3 ± 13.5	63.6 ± 9.1	0.080
Disease-specific characteristics			
Duration of psoriasis, year	17.3 ± 14.5		
Duration of PsA, year	13.1 ± 7.2		
Nail involvement, %	44 (68.8)		
CRP, mg/L	5.2 ± 8.4		
ESR, mm/h	20.5 ± 20.6		
DAPSA	10.8 ± 8.11		
PASI	6.8 ± 9.8		
HAQ	0.3 (0, 0.6)		
VAS pain, mm	31.3 ± 26.2		
VAS PhyGA, mm	22.5 ± 21.2		
VAS PatGA, mm	43.6 ± 28.1		
Tender joint count	0 (0, 2)		
Swollen joint count	0 (0, 0)		
Deformed joint count	1 (0, 4)		
Current treatment			
Corticosteroids, %	3 (4.8)		
Any DMARDs, %	37 (59.7)		
csDMARDs, %	33 (53.2)		
bDMARDs, %	11 (17.7)		
csDMARDs+bDMARDs, %	7 (11.3)		

Results are mean ± SD or median (interquartile range) for continuous data and number (percentage) for categoric data unless otherwise indicated. *PsA*, psoriatic arthritis; *JD*, joint destruction; *BMI*, body mass index; *CRP*, C-reactive protein; *ESR*, erythrocyte sedimentation rate; *DAPSA*, disease activity in psoriatic arthritis; *PASI*, Psoriasis Area and Severity Index; *HAQ*, Health Assessment Questionnaire; *VAS*, Visual Analogue Scale; *PhyGA*, physician global assessment; *PatGA*, patient global assessment; *csDMARDs*, conventional synthetic disease-modifying anti-rheumatic drugs; *bDMARDs*, biologic disease-modifying anti-rheumatic drugs; * denotes comparison between PsA with and without JD; [#] denotes comparison between PsA without JD and control

Table 2 Number and size of erosions and enthesiophytes in psoriatic arthritis (PsA) patients and controls

Number	PsA ($n = 62$)	Controls ($n = 62$)	p value
Erosions total, *n*	85	50	
Erosion mean, *n*	1.4 ± 1.2	1.1 ± 1.0	0.110
Metacarpal head 2, *n* (%)	42 (49)	24 (48)	
Metacarpal head 3, *n* (%)	43 (51)	26 (52)	
Enthesiophytes total, *n*	150	80	
Enthesiophyte mean, *n*	2.4 ± 1.4	1.3 ± 1.1	*0.000*
Metacarpal head 2, *n* (%)	84 (56)	57 (71)	
Metacarpal head 3, *n* (%)	66 (44)	23 (29)	
Total volume of erosion per person, mm^3	5.2 ± 6.0	2.8 ± 4.5	*0.003*
Total height of enthesiophyte per person, mm	2.5 ± 1.6	1.4 ± 1.3	*0.000*
Total volume of enthesiophyte per person, mm^3	8.8 ± 7.0	4.4 ± 4.9	*0.000*

Results are mean ± SD or number (percentage) unless otherwise indicated. Volume and height (target erosion and enthesiophyte) are the sum of the measures obtained in each quadrant for each compartment at second and third metacarpal head. Significant results are highlighted in italics

the PsA group. At MCH 2&3, the number (mean number per patient 2.4 ± 1.4 vs 1.3 ± 1.1, $p = 0.000$), height (PsA: 2.5 ± 1.6 mm vs control: 1.4 ± 1.3 mm, $p = 0.000$), and volume (PsA: 8.8 ± 7.0 mm^3 vs control: 4.4 ± 4.9 mm^3, $p = 0.000$) of enthesiophytes in PsA patients were greater than controls (Table 2). Enthesiophytes had a predilection for the palmar

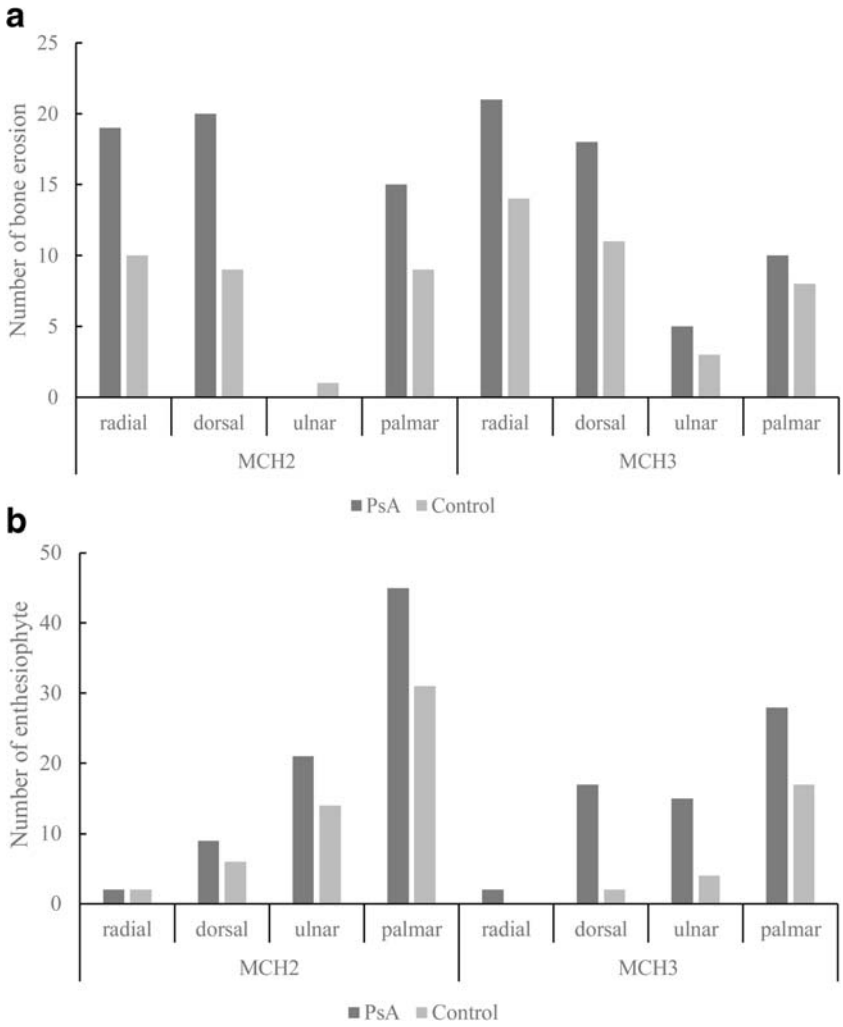

Fig. 2 Anatomic distribution of bone erosion and enthesiophyte. Number and quadrant of bone erosion in PsA patients and healthy controls (A). Number and quadrant of enthesiophyte in PsA patients and healthy controls (B). The metacarpal head was divided into palmar, ulnar, dorsal, and radial quadrants. MCH metacarpal head, PsA psoriatic arthritis, Ctrl healthy control

sites (Fig. 2B). In PsA patients, older age correlated with larger erosion and enthesiophyte volume (sTable 1).

Comparison of vBMD and microstructure at the second and third metacarpal head in PsA and controls

Table 3 summarizes the mean vBMD and microstructure at MCH 2&3. Significantly lower mean vBMD (average vBMD: −6.9%, $p = 0.007$, Tb vBMD: −8.8%, $p < 0.001$, pTb vBMD: −7.7%, $p = 0.001$, mTb vBMD: −9.8%, $p < 0.001$), average BV/TV (−8.8%, $p < 0.001$), and average Tb thickness (−8.1%, $p = 0.003$) were observed at the MCH 2&3 in PsA patients compared with control subjects (Table 3). Multivariable linear regression analysis revealed that older age and a higher CRP level were independently associated with lower mean vBMD (average, Tb, and mTb) and average BV/TV at MCH 2&3 (Table 4).

Discussion

The study quantitatively and simultaneously compares the bone structure and microstructure in the metacarpal head between PsA patients and age-, gender-, and BMI-matched healthy control. To achieve this aim, we quantified both enthesiophyte and bone erosion volume, and assessed vBMD and microstructure after exclusion of bone erosion and enthesiophyte. The methodology for measuring erosion volume was modified for the quantification of enthesiophyte volume in the current study, and we have shown that this was feasible and reliable.

In line with the only study addressing structural bone damage in PsA patients compared with control subjects [8], we found larger bone erosion and enthesiophyte volume and more enthesiophytes in PsA patients than control subjects. Similar to previous study [7, 8], enthesiophytes are more common in PsA compared with control, supporting the hypothesis that PsA is predominantly an enthesitis-driven disease. Unfortunately, only a small number of HR-pQCT studies showed that IL-17 inhibition might halt the progression of both erosion and enthesiophytes [10]. The anatomic distribution of bone erosion and enthesiophyte was consistent with previous HR-pQCT studies for patients with PsA and psoriasis patients without PsA [4, 7].

Contrary to the only other HR-pQCT-based study comparing PsA patients and control subjects, which did not show any differences in bone microarchitecture between PsA patients and control subjects [33], our study found that mean average vBMD, peripheral and medullary trabecular vBMD, and trabecular bone volume fraction at MCH 2&3 were significantly decreased in patients with PsA compared with healthy control subjects. This discrepancy may be related to a shorter PsA disease duration (4.6 ± 6.4 years) of the previous study as well as the methodology used [33]. While erosions were excluded during analysis in the previous study, enthesiophytes were not excluded. The inclusion of enthesiophytes would clearly increase perceived cortical bone density. In addition, the previous study deployed a technique based on contouring the metacarpal head to adapt the number of slices rather than using a pre-determined, fixed number of slices as in the present study [11, 33].

In patients with PsA, this study suggests that inflammation might aggravate trabecular bone loss in the intra-articular metacarpal bone. Data from this study demonstrated that in

Table 3 Comparison of mean vBMD and microstructure at the second and third metacarpal heads in PsA patients and controls

	PsA	Control	*p* value	Diff (%)
Average vBMD, mg HA/cm^3	284.37 ± 42.57	305.33 ± 42.02	*0.007*	*− 6.9*
Ct. vBMD, mg HA/cm^3	536.97 ± 72.28	547.68 ± 72.84	0.413	− 2.0
Tb. vBMD, mg HA/cm^3	224.06 ± 35.32	245.75 ± 29.72	*0.000*	*− 8.8*
pTb. vBMD, mg HA/cm^3	258.95 ± 37.71	280.44 ± 35.39	*0.001*	*− 7.7*
mTb. vBMD, mg HA/cm^3	199.52 ± 36.58	221.28 ± 30.67	*0.000*	*− 9.8*
BV/TV, %	0.19 ± 0.03	0.20 ± 0.02	*0.000*	*− 8.8*
Tb. number, mm^{-1}	1.92 ± 0.25	1.95 ± 0.29	0.601	− 1.3
Tb. thickness, mm	0.10 ± 0.02	0.11 ± 0.02	*0.003*	*− 8.1*
Tb. separation, mm	0.43 ± 0.07	0.42 ± 0.08	0.349	2.9
Inhomogeneity, mm	0.25 ± 0.07	0.24 ± 0.08	0.763	1.7
Ct. thickness, mm	21.02 ± 1.19	20.65 ± 1.37	0.113	1.8
Ct. perimeter, mm	42.57 ± 3.28	41.58 ± 3.88	0.125	2.4

Results are mean ± SD. *PsA*, psoriatic arthritis; *vBMD*, volumetric bone mineral density; *Ct*, cortical; *Tb*, trabecular; *pTb*, peripheral trabecular (trabecular bone in the peripheral region adjacent to the cortex); *mTb*, medullary trabecular (trabecular bone in the central medullary region); *BV/TV*, trabecular bone volume fraction; differences (%) were calculated using the following formula: PsA vs control (Ctrl) = (PsA − Ctrl)/Ctrl; *$p < 0.05$; **$p < 0.01$; significant results are highlighted in italics

Table 4 Univariate and multivariable analysis for mean vBMD and microstructure at the second and third metacarpal head in PsA patients

	Age	BMI	PsO duration	PsA duration	CRP	DAPSA
	Correlation coefficient					
Average vBMD, mg HA/cm^3	− 0.173*	0.069	− 0.010	− 0.029	− 0.309**	− 0.162
Tb. vBMD, mg HA/cm^3	− 0.182*	0.045	− 0.049	− 0.024	− 0.255*	− 0.226
pTb. vBMD, mg HA/cm^3	− 0.245**	0.054	− 0.060	− 0.025	− 0.310**	− 0.208
mTb.vBMD, mg HA/cm^3	− 0.115	0.032	− 0.037	− 0.021	− 0.196*	− 0.222
BV/TV, %	− 0.182*	0.045	− 0.048	− 0.024	− 0.255*	− 0.225
Tb. thickness, mm	− 0.230*	0.028	− 0.045	− 0.107	− 0.148	− 0.161
	Multivariable analysis (regression coefficient)					
Average vBMD, mg HA/cm^3					− 1.232	
Tb. vBMD, mg HA/cm^3	− 1.143					
pTb. vBMD, mg HA/cm^3	− 1.135				− 1.259	
mTb.vBMD, mg HA/cm^3					− 1.059	
BV/TV, %	− 0.001				− 0.001	
Tb. thickness, mm	0.001					

Results are presented as correlation coefficients for univariate analysis, or as regression coefficients for multivariable analysis, only independent explanatory variables in the multivariable analysis were shown. *BMI*, body mass index; *PsA*, psoriatic arthritis; *PsO*, psoriasis; *CRP*, C-reactive protein; *DAPSA*, disease activity in psoriatic arthritis; *HAQ*, Health Assessment Questionnaire; *vBMD*, volumetric bone mineral density; *Tb*, trabecular; *pTb*, peripheral trabecular (trabecular bone in the peripheral region adjacent to the cortex); *mTb*, medullary trabecular (trabecular bone in the central medullary region); *BV/TV*, trabecular bone volume fraction; * denotes $p < 0.05$, ** denotes $p < 0.01$

patients with PsA, deterioration in average vBMD and predominantly trabecular vBMD (and trabecular bone volume fraction which was derived from trabecular vBMD) were significantly associated with an increased CRP level, which provided preliminary evidence to suggest that inflammation may contribute to bone loss in PsA patients. However, multivariable analysis did not find any association between the CRP level and trabecular number and separation in our PsA cohort, which is consistent with our previous study in a group of patients with RA [34]. Whether and how inflammation accelerates loss of trabeculae in PsA would need to be addressed in future studies. Similarly, we did not observe any association between CRP level and the volume of enthesiophyte and erosion. Duration of PsA was reported to be significantly correlated with the burden of enthesiophytes and erosions in a previous study which included patients with a shorter disease duration (mean PsA duration of 6.4 years compared with 13.1 years in the current study) [8]. These bony damages reflect accumulating mechanical and inflammatory damage in the joints. The inflammatory burden may not be captured in a snapshot provided by the single CRP level. The effects of inflammation accelerating bone damage may be more prominent in patients with shorter disease duration and therefore even disease duration was not identified as an explanatory variable associated with bone damages in our cohort.

Our findings revealed decreased average and trabecular vBMD but not cortical vBMD in metacarpal head in PsA patients, which might be explained by the absence of anti-citrullinated protein antibody (ACPA) in PsA. In ACPA-positive healthy individuals compared with ACPA-negative healthy individuals without clinical signs of arthritis, bone loss tends to affect the cortical but not trabecular compartment of the metacarpal head [35]. Similarly, compared with healthy control subjects, ACPA-positive RA patients had significantly reduced cortical and trabecular vBMD [11, 33], though only decreased trabecular vBMD is seen in RA patients with fewer ACPA-positive patients [36].

There are a few limitations to our study. First, almost one-fifth (19.5%) of PsA patients with joint destruction were excluded from structural and microstructural analysis as hand positioning and image analysis can be difficult in patients with severe joint deformity. Second, the cross-sectional design could only establish an association between clinical characteristics and bone damage, but not a causal effect relationship. Future longitudinal study is needed to confirm the effect of inflammation on structural and microstructural bone change.

In conclusion, the burden of bone erosions, enthesiophytes, and trabecular bone loss is increased in PsA patients compared with matched healthy controls. PsA patients had a predominant deterioration in trabecular microstructure in the metacarpal head which was related to ongoing disease inflammation.

Acknowledgments We thank all patients who participated in this study.

Compliance with ethical standards Ethics approval (CRE-2012.082) was obtained from the Ethics Committee of The Chinese University of Hong Kong-New Territories East Cluster Hospitals with written informed consent obtained from all participants.

Conflicts of interest None.

References

1. Moll JM, Wright V (1973) Psoriatic arthritis. Semin Arthritis Rheum 3:55–78
2. Gladman DD, Antoni C, Mease P, Clegg DO, Nash P (2005) Psoriatic arthritis: epidemiology, clinical features, course, and outcome. Ann Rheum Dis 64 Suppl 2:ii14–ii17
3. Ritchlin CT, Colbert RA, Gladman DD (2017) Psoriatic arthritis. N Engl J Med 376:957–970
4. Finzel S, Englbrecht M, Engelke K, Stach C, Schett G (2011) A comparative study of periarticular bone lesions in rheumatoid arthritis and psoriatic arthritis. Ann Rheum Dis 70:122–127
5. Finzel S, Sahinbegovic E, Kocijan R, Engelke K, Englbrecht M, Schett G (2014) Inflammatory bone spur formation in psoriatic arthritis is different from bone spur formation in hand osteoarthritis. Arthritis Rheum 66:2968–2975
6. Geusens P, Chapurlat R, Schett G, Ghasem-Zadeh A, Seeman E, de Jong J, van den Bergh J (2014) High-resolution in vivo imaging of bone and joints: a window to microarchitecture. Nat Rev Rheumatol 10:304–313
7. Simon D, Faustini F, Kleyer A, Haschka J, Englbrecht M, Kraus S, Hueber AJ, Kocijan R, Sticherling M, Schett G, Rech J (2016) Analysis of periarticular bone changes in patients with cutaneous psoriasis without associated psoriatic arthritis. Ann Rheum Dis 75: 660–666
8. Simon D, Kleyer A, Faustini F et al (2018) Simultaneous quantification of bone erosions and enthesiophytes in the joints of patients with psoriasis or psoriatic arthritis - effects of age and disease duration. Arthritis Res Ther 20:203
9. Finzel S, Kraus S, Schmidt S, Hueber A, Rech J, Engelke K, Englbrecht M, Schett G (2013) Bone anabolic changes progress in psoriatic arthritis patients despite treatment with methotrexate or tumour necrosis factor inhibitors. Ann Rheum Dis 72:1176–1181
10. Kampylafka E, d'Oliveira I, Linz C et al (2018) Resolution of synovitis and arrest of catabolic and anabolic bone changes in patients with psoriatic arthritis by IL-17A blockade with secukinumab: results from the prospective PSARTROS study. Arthritis Res Ther 20:153
11. Simon D, Kleyer A, Stemmler F et al (2017) Age- and sex-dependent changes of intra-articular cortical and trabecular bone structure and the effects of rheumatoid arthritis. J Bone Miner Res 32:722–730
12. Zhu TY, Griffith JF, Qin L, Hung VW, Fong TN, Au SK, Kwok AW, Leung PC, Li EK, Tam LS (2015) Density, structure, and strength of the distal radius in patients with psoriatic arthritis: the role of inflammation and cardiovascular risk factors. Osteoporos Int 26:261–272
13. Taylor W, Gladman D, Helliwell P, Marchesoni A, Mease P, Mielants H, Group CS (2006) Classification criteria for psoriatic arthritis: development of new criteria from a large international study. Arthritis Rheum 54:2665–2673
14. Stach CM, Bauerle M, Englbrecht M, Kronke G, Engelke K, Manger B, Schett G (2010) Periarticular bone structure in rheumatoid arthritis patients and healthy individuals assessed by high-resolution computed tomography. Arthritis Rheum 62:330–339
15. Aletaha D, Alasti F, Smolen JS (2017) Disease activity states of the DAPSA, a psoriatic arthritis specific instrument, are valid against functional status and structural progression. Ann Rheum Dis 76: 418–421
16. Scharmga A, Peters M, van den Bergh JP, Geusens P, Loeffen D, van Rietbergen B, Schoonbrood T, Vosse D, Weijers R, van Tubergen A (2018) Development of a scoring method to visually score cortical interruptions on high-resolution peripheral quantitative computed tomography in rheumatoid arthritis and healthy controls. PLoS One 13:e0200331
17. Scharmga A, Peters M, van Tubergen A, van den Bergh J, Barnabe C, Finzel S, van Rietbergen B, Geusens P (2016) Heterogeneity of cortical breaks in hand joints of patients with rheumatoid arthritis and healthy controls imaged by high-resolution peripheral quantitative computed tomography. J Rheumatol 43:1914–1920
18. Boutroy S, Chapurlat R, Vanden-Bossche A, Locrelle H, Thomas T, Marotte H (2015) Erosion or vascular channel? Arthritis Rheum 67:2956
19. Scharmga A, Keller KK, Peters M, van Tubergen A, van den Bergh JP, van Rietbergen B, Weijers R, Loeffen D, Hauge EM, Geusens P (2017) Vascular channels in metacarpophalangeal joints: a comparative histologic and high-resolution imaging study. Sci Rep 7:8966
20. Finzel S, Ohrndorf S, Englbrecht M, Stach C, Messerschmidt J, Schett G, Backhaus M (2011) A detailed comparative study of high-resolution ultrasound and micro-computed tomography for detection of arthritic bone erosions. Arthritis Rheum 63:1231–1236
21. Faustini F, Simon D, Oliveira I, Kleyer A, Haschka J, Englbrecht M, Cavalcante AR, Kraus S, Tabosa TP, Figueiredo C, Hueber AJ, Kocijan R, Cavallaro A, Schett G, Sticherling M, Rech J (2016) Subclinical joint inflammation in patients with psoriasis without concomitant psoriatic arthritis: a cross-sectional and longitudinal analysis. Ann Rheum Dis 75:2068–2074
22. Yushkevich PA, Yang G, Gerig G (2016) ITK-SNAP: an interactive tool for semi-automatic segmentation of multi-modality biomedical images. Conference Proc 2016:3342–3345
23. Yushkevich PA, Gerig G (2017) ITK-SNAP: an intractive medical image segmentation tool to meet the need for expert-guided segmentation of complex medical images. IEEE Pulse 8:54–57
24. Yushkevich PA, Piven J, Hazlett HC, Smith RG, Ho S, Gee JC, Gerig G (2006) User-guided 3D active contour segmentation of anatomical structures: significantly improved efficiency and reliability. NeuroImage 31:1116–1128
25. Vallaeys K, Kacem A, Legoux H, Le Tenier M, Hamitouche C, Arbab-Chirani R (2015) 3D dento-maxillary osteolytic lesion and active contour segmentation pilot study in CBCT: semi-automatic vs manual methods. Dento Maxillo Facial Radiol 44:20150079
26. Besson FL, Henry T, Meyer C et al (2018) Rapid contour-based segmentation for (18)F-FDG PET imaging of lung tumors by using ITK-SNAP: comparison to expert-based segmentation. Radiology 288:277–284
27. Akudjedu TN, Nabulsi L, Makelyte M et al (2018) A comparative study of segmentation techniques for the quantification of brain subcortical volume. Brain Imaging Behav 12:1678–1695
28. Lu P, Barazzetti L, Chandran V, Gavaghan K, Weber S, Gerber N, Reyes M (2018) Highly accurate facial nerve segmentation refinement from CBCT/CT imaging using a super-resolution classification approach. IEEE Trans Biomed Eng 65:178–188
29. Lories RJ, Schett G (2012) Pathophysiology of new bone formation and ankylosis in spondyloarthritis. Rheum Dis Clin N Am 38:555–567
30. Boutroy S, Bouxsein ML, Munoz F, Delmas PD (2005) In vivo assessment of trabecular bone microarchitecture by high-resolution peripheral quantitative computed tomography. J Clin Endocrinol Metab 90:6508–6515
31. Yang H, Yu A, Burghardt AJ, Virayavanich W, Link TM, Imboden JB, Li X (2017) Quantitative characterization of metacarpal and

radial bone in rheumatoid arthritis using high resolution-peripheral quantitative computed tomography. Int J Rheum Dis 20:353–362
32. Zhu TY, Griffith JF, Qin L et al (2013) Structure and strength of the distal radius in female patients with rheumatoid arthritis: a case-control study. J Bone Miner Res 28:794–806
33. Simon D, Kleyer A, Englbrecht M, Stemmler F, Simon C, Berlin A, Kocijan R, Haschka J, Hirschmann S, Atreya R, Neurath MF, Sticherling M, Rech J, Hueber AJ, Engelke K, Schett G (2018) A comparative analysis of articular bone in large cohort of patients with chronic inflammatory diseases of the joints, the gut and the skin. Bone 116:87–93
34. Zhu TY, Griffith JF, Qin L, Hung VW, Fong TN, Kwok AW, Leung PC, Li EK, Tam LS (2012) Bone density and microarchitecture: relationship between hand, peripheral, and axial skeletal sites assessed by HR-pQCT and DXA in rheumatoid arthritis. Calcif Tissue Int 91:343–355
35. Kleyer A, Finzel S, Rech J, Manger B, Krieter M, Faustini F, Araujo E, Hueber AJ, Harre U, Engelke K, Schett G (2014) Bone loss before the clinical onset of rheumatoid arthritis in subjects with anticitrullinated protein antibodies. Ann Rheum Dis 73:854–860
36. Fouque-Aubert A, Boutroy S, Marotte H, Vilayphiou N, Bacchetta J, Miossec P, Delmas PD, Chapurlat RD (2010) Assessment of hand bone loss in rheumatoid arthritis by high-resolution peripheral quantitative CT. Ann Rheum Dis 69:1671–1676